

Compositionally Complex Alloy MnFeCoNiCu for Brazing Nickel-Based Superalloy Haynes 214

Jonas Vogler, Benjamin Schneiderman, Zhenzhen Yu, Jakob Huber, Rainer Völkl, and Uwe Glatzel*

The microstructural and mechanical properties of a MnFeCoNiCu braze filler are analyzed and compared to a conventional nickel-based braze filler alloy on Haynes 214 as the base material. Tensile tests reveal that the samples brazed with the MnFeCoNiCu compositionally complex alloy (CCA) exhibit superior ductility increased by a factor of 1.6 compared to those brazed with the nickel-based filler. The ultimate tensile strength remains comparable (factor 1.03). Contact angles recorded during the brazing process indicate comparable wetting properties between the two fillers. Based on experimental investigations and Thermo-Calc predictions, improved brazing parameters are proposed for the CCA filler on Haynes 214. These recommendations include lower brazing temperatures, shortened holding times, and faster cooling rates.

designed to provide effective sealing and prevent leakage of gases between the rotor and stator.^[1] Honeycomb sealing systems brazed with nickel-based braze filler alloys exhibit good resistance to high temperatures, corrosion, and mechanical stresses. A typical base material used is Haynes 214, an alumina-forming nickel-based superalloy.^[2,3]

Using the transient liquid-phase bonding process with filler materials containing boron or silicon as liquidus temperature depressants is a common approach to achieve robust brazed joints. The nickel-based filler alloy BNi-5^[4] is commonly used in high-temperature applications. However, a significant drawback of the transient

1. Introduction

Vacuum brazing is a widely used joining technique in the manufacturing and assembly of honeycomb sealing systems. Honeycomb structures, known for their excellent strength-to-weight ratio and high thermal and mechanical stability, find extensive applications in turbine engines. These systems are

liquid-phase bonding method is precipitation of a brittle phase in the microstructure due to eutectic solidification after an insufficient holding time at brazing temperature, leading to limited ductility and potentially compromising the overall mechanical properties and lifetime of the brazed components.^[5–8]

In the standard process for manufacturing honeycomb seals, metal sheets are corrugated into a semi-hexagonal shape. These bent metal sheets are then assembled to form a hexagonal shape. They are subsequently spot welded and brazed onto a base plate. As a result of capillary forces, the liquid braze filler flows to the top surface along edges and double-foil sections.^[9] The presence of brittle phases within the filler has the potential to detrimentally impact rubbing properties. These particles may contribute to elevated thermal and mechanical loads, thereby increasing the probability of rotor damage.


To suppress brittle phases, a novel MnFeCoNiCu compositionally complex alloy (CCA) filler was developed and implemented, targeting a single-phase solidification mechanism resulting in a face-centered-cubic (FCC) solid-solution phase.^[10–12] This CCA was designed to have an appropriate liquidus temperature of 1100 °C for brazing superalloys used in high-temperature applications, eliminating the need for additional liquidus-temperature modifiers.

J. Vogler, R. Völkl, U. Glatzel
Metals and Alloys
University of Bayreuth
Prof.-Rüdiger-Bormann-Straße 1, Bayreuth 95447, Germany
E-mail: uwe.glatzel@uni-bayreuth.de

B. Schneiderman, Z. Yu
Department of Metallurgical and Materials Engineering
Colorado School of Mines
1500 Illinois St., Golden, CO 80401, USA

B. Schneiderman, Z. Yu
HYSA Fillers
1600 Jackson St., Golden, CO 80401, USA

J. Huber
Chair of Materials Science
Technical University of Munich
Boltzmannstr. 15, 85748 Garching, Germany

 The ORCID identification number(s) for the author(s) of this article can be found under <https://doi.org/10.1002/adem.202400747>.

© 2024 The Author(s). Advanced Engineering Materials published by Wiley-VCH GmbH. This is an open access article under the terms of the Creative Commons Attribution License, which permits use, distribution and reproduction in any medium, provided the original work is properly cited.

DOI: 10.1002/adem.202400747

2. Experimental Section

Table 1 lists the materials used: Haynes 214 as base material and CCA and BNi-5 compound as filler materials. The CCA filler was provided by HYSA Fillers. It had a similar composition to that employed by Schneiderman et al.^[11] and Gao et al.^[12]

Table 1. Liquidus temperature T_m as determined in results section and nominal composition of Haynes 214, BNi-5 and the CCA filler in wt%.^[2,4,12]

Element	Ni	Cr	Si	Al	Fe	Mn	Mo, Ti, W	Co	Cu	T_m [°C]
Material										
Haynes 214	75 Bal.	16	<0.2	4.5	3	<0.5	<0.5	<2	–	1400
BNi-5 (AMS 4782)	71 Bal.	19	10	–	–	–	–	–	–	1135
CCA	20	–	–	–	5	33	–	20	22	1105

The Haynes 214 metal sheets were delivered with a thickness of 0.29 mm.

Brazing with the CCA braze filler alloy was conducted at a holding temperature of 1200 °C. CCA braze samples were prepared with two different cooling rates and hold durations. The fast-cooled sample exhibited an average cooling rate of 110 °C min^{−1} from 1200 to 600 °C and a hold duration at 1200 °C of 60 min. In contrast, the slow-cooled sample had a cooling rate of 10 °C min^{−1} during the same temperature interval and a hold duration of 90 min. The CCA was applied as brazing foil with an original thickness of 0.13 mm, placed in between two 28 × 40 mm pieces of Haynes 214 sheet. The area of brazing foil used was calculated as that which would achieve a filler thickness of ≈40 μm after spreading uniformly across the substrate, with spreading assisted by applying a load of 1 N to the metal sheets.

The BNi-5 samples were brazed at 1170 °C with a holding time of 15 min and a cooling rate of 5.5 °C min^{−1} from 1170 to 900 °C and 20 °C min^{−1} from 900 °C to room temperature. The brazing foil initially measured 40 μm in thickness, prompting the use of a piece matching the substrate's dimensions to ensure that the final braze thickness remained at 40 μm. **Table 2** lists all crucial parameters of the various brazing processes examined in this study.

Microstructure studies were carried out using scanning electron microscopy, element distribution analysis was performed by energy-dispersive X-ray spectroscopy (EDX), and grain sizes were determined using electron backscattering diffraction (EBSD) on a Zeiss Sigma 300 VP and Zeiss 1540 EsB Cross Beam.

Tensile tests were conducted on brazed thin sheets of Haynes 214 with the plane of the braze oriented parallel to the tensile axis. Specimens were extracted with electrical discharge machining. The tests were performed on a Zwick Z2.5 universal testing machine at a strain rate of about 10^{−2} s^{−1}.

An analysis of the wetting kinetics of the braze filler alloys on Haynes 214 substrates was conducted to optimize brazing parameters and ensure uniform filler material distribution. An in situ contact angle measurement system was developed to

assist in the optimization of the brazing parameters, allowing real-time analysis of the temperature and time-dependent contact angles at test temperatures up to 2000 °C. For the wettability tests, cubes of the braze filler alloys (BNi-5 and CCA filler) with a volume of 2 × 2 × 2 mm³ weighing ≈0.06 g were melted on Haynes 214 metal sheets with an area size of 28 × 20 mm². The melting process was recorded in a video at a frame rate of 1 frame per second. Contact angle and drop volume were measured using the Python program drop analysis by van Gorcum.^[13] The program was adapted to the experimental setup to measure the dependency of contact angle on temperature and time.

To investigate whether the alloying elements in the CCA braze filler affected its oxidation properties postbrazing, oxidation experiments were conducted at 1000 °C for 168 h in air. Three brazed samples with a size of 12 × 40 mm² and with a thickness of ≈0.62 mm were assessed; the mass gain associated with oxidation was quantified.

The solidus and liquidus temperatures of the CCA filler were estimated using Thermo-Calc simulations^[14] with the TCNI12 database. The melting temperature simulation results were validated using differential scanning calorimetry (DSC) on a NETZSCH STA 449F3 with a heating rate of 20 °C min^{−1} and a cooling rate of 10 °C min^{−1}. Additionally, the diffusion behavior of the CCA during the brazing process was simulated, employing the mobility database MOBNI6 and the upper Wiener-bound homogenization function. The diffusion simulations encompassed a 300 μm-thick Haynes 214 area and a 50 μm-thick filler area. To enhance computational efficiency, FCC matrix phase and liquid phase were included in the simulation. The simulated diffusion profiles were compared to those determined experimentally through EDX measurements.

3. Results

3.1. Melting Temperature Simulation

Figure 1 shows the results of the Thermo-Calc material-to-material simulation (linear transition from 100 wt% CCA filler to 100 wt% Haynes 214). The simulations predict a solidus temperature of 1060 °C and a liquidus temperature of 1110 °C for the CCA filler. The liquidus temperature of 1395 °C for Haynes 214 is in good agreement with the datasheet value of 1400 °C.^[2] Up to a Haynes 214 fraction of 20%, the liquidus and solidus temperatures show only minimal changes. Beyond this point, both temperatures consistently increase.

Table 2. Brazing processes performed in this study.

Brazing process	Materials	Brazing temperature [°C]	Holding time [min]	Cooling rate to below 600 °C [°C min ^{−1}]
Fast cooling	Haynes 214 + CCA	1200	60	110
Slow cooling	Haynes 214 + CCA	1200	90	10
Conventional	Haynes 214 + BNi-5	1170	15	20

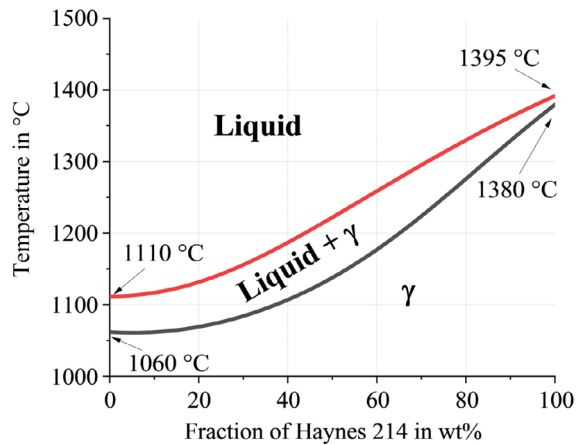


Figure 1. Liquidus and solidus temperatures as predicted by Thermo-Calc material-to-material simulation. Linear transition from 100% CCA filler to 100% Haynes 214.

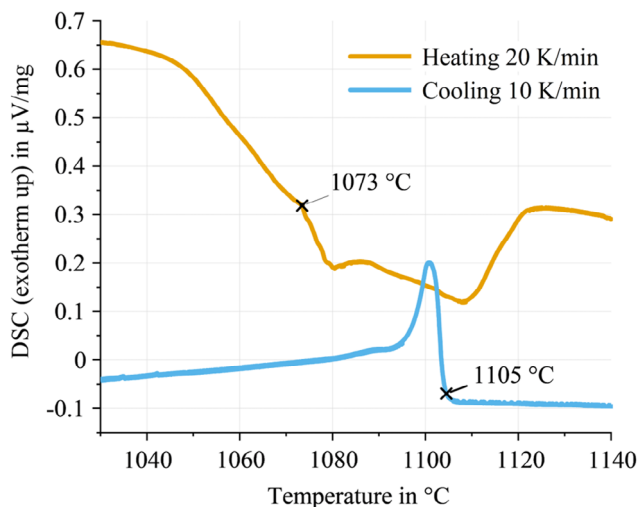


Figure 2. Cooling and heating curves from the DSC measurement of the CCA filler.

Figure 2 shows the outcomes from DSC measurements, providing experimental values for the liquidus and solidus temperatures of the novel CCA filler. The heating curve (orange) shows a solidus temperature of ≈ 1073 °C since the sharp change in slope at this location indicates the onset of latent heat absorption. The cooling curve (blue) shows a liquidus temperature of around 1105 °C.

3.2. Microstructures

Figure 3 shows the EDX images of nickel, copper, and manganese after the slow-cooling brazing process. No manganese- or copper-rich precipitates are visible with a resolution of ≈ 5 μm .

Figure 4 shows the average of five linescans perpendicular to the brazing centerline.

No phases are visible in the EDX mappings (resolution of 1 μm) of the diffusion zone after the slow-cooling brazing process (**Figure 3**). Furthermore, the absence of peaks and the homogeneous concentration profile of the CCA constituent elements in various elemental line scans (**Figure 4**) show that the diffusion zone is a single-phase solid solution. The diffusion-affected zones of Co and Cu exhibit similar characteristics, both of them about 230 μm wide. In contrast, the diffusion-affected zone of Mn is broader, measuring 330 μm , indicating a 100 μm difference compared to Co and Cu. This is consistent with a prior study on the diffusion of Co, Cu, and Mn into a nickel alloy, which concluded that Mn diffuses the furthest, but its diffusivity is significantly reduced in the presence of the other CCA elements in comparison to a Ni–Mn binary couple.^[12] The distribution of iron is uniform, since no areas with increased concentrations are detected. A zone with a nickel content smaller than 71 wt% extends up to 340 μm . The chromium-depleted zone (< 16 wt%) has a width of 260 μm . At its center, the chromium content reaches a minimum of 9.5 wt%.

Figure 5 shows the simulation data from Thermo-Calc diffusion experiments (dots) together with experimentally determined diffusion profiles for the fast-cooled brazing process (solid lines). Only the three elements, Mn, Cr, and Al, are represented to enhance clarity. The simulated diffusion profiles closely align with the experimentally obtained values for all elements. Only the diffusion into the left Haynes 214 metal sheet was simulated to reduce computation time.

Figure 6 shows the EDX images of nickel, copper, and manganese after the fast-cooling brazing process. The diffusion zones after the fast-cooling brazing process are noticeably smaller compared to the diffusion zones after the slow-cooling process. For instance, in the case of Mn, this distance is only about 250 μm (see **Figure 5** and **6**). Additionally, the concentration differences are significantly larger. Along the brazing centerline, a manganese- and copper-rich segregation is observed, as evidenced by the small peak in **Figure 5** at 0 μm and affirmed by the EDX images in **Figure 6**.

Figure 7 shows two EBSD grain orientation images. These images were obtained after undergoing the two different CCA brazing processes: 1200 °C for 60 min (fast cooled) and 1200 °C for 90 min (slow cooled).

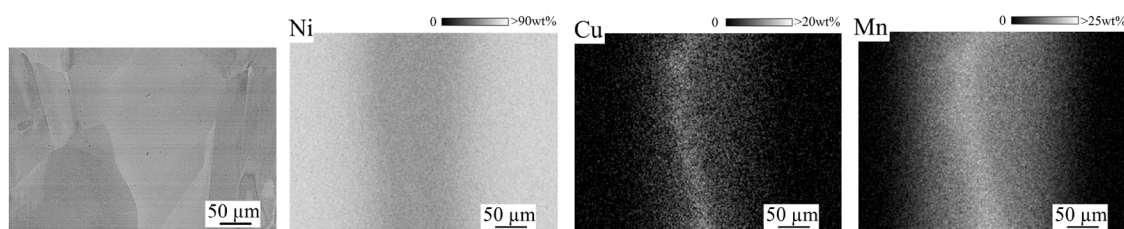


Figure 3. EDX mappings and backscattered electron image in the brazing joint region after the CCA brazing process at 1200 °C for 90 min (slow-cooling).

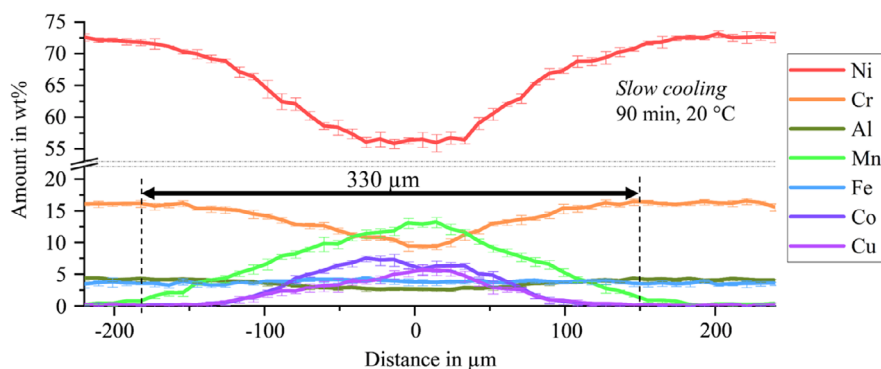


Figure 4. Line-scan of the CCA brazing joint area after brazing at 1200 °C for 90 min. Mean values and standard deviation are obtained from five measurements. The range between 25 and 50 wt% has been cropped for a clearer representation of the line-scans.

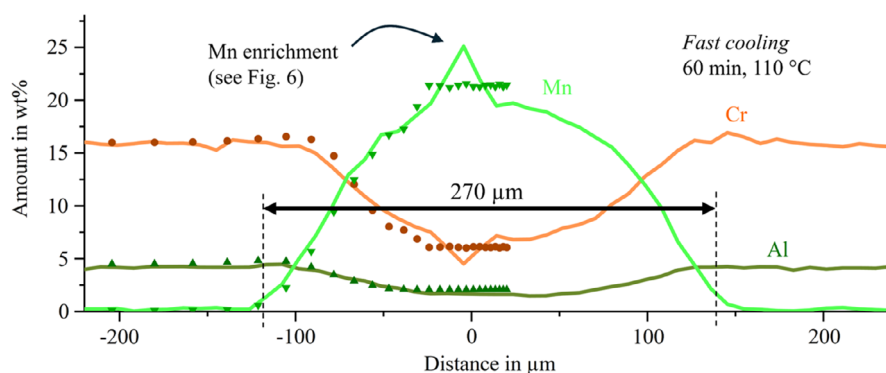


Figure 5. Average of five line-scans after brazing with the CCA filler at 1200 °C for 60 min (solid line) and results from the Thermo-Calc diffusion simulation (dots).

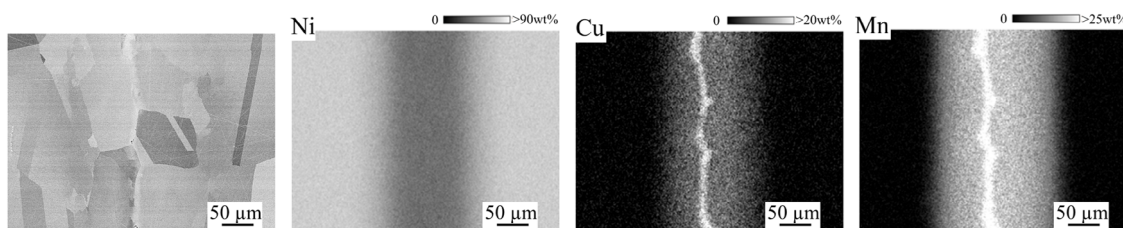


Figure 6. EDX mappings and backscattered electron image in the brazing joint region after the CCA brazing process at 1200 °C for 60 min (fast-cooling).

The initial Haynes 214 metal sheets exhibit an equiaxed grain structure with an average grain size of 30 μm .^[5] Following the brazing process with BNi-5, the average grain size increases strongly to 330 μm .^[5]

Interestingly, the average grain size of the CCA-brazed sample is smaller despite higher brazing temperatures. After the fast-cooled brazing process at 1200 °C for 60 min, the average grain size is 220 μm . The formation of smaller grains is visible in Figure 7a close to the joint area. However, these smaller grains at the braze joint are not observed in Figure 7b in the slow-cooled condition. For this specimen, the grain size is more uniform and

slightly larger with $\approx 250 \mu\text{m}$. Faster cooling results in less time for recrystallization.

3.3. Mechanical Properties

Figure 8 shows stress–strain curves obtained at a strain rate of 10^{-2} s^{-1} and at room temperature.

A total of five experiments were conducted per sample. The mean value and standard deviation for each sample are presented in Table 3. The CCA-brazed samples show higher ductility than those brazed with the conventional

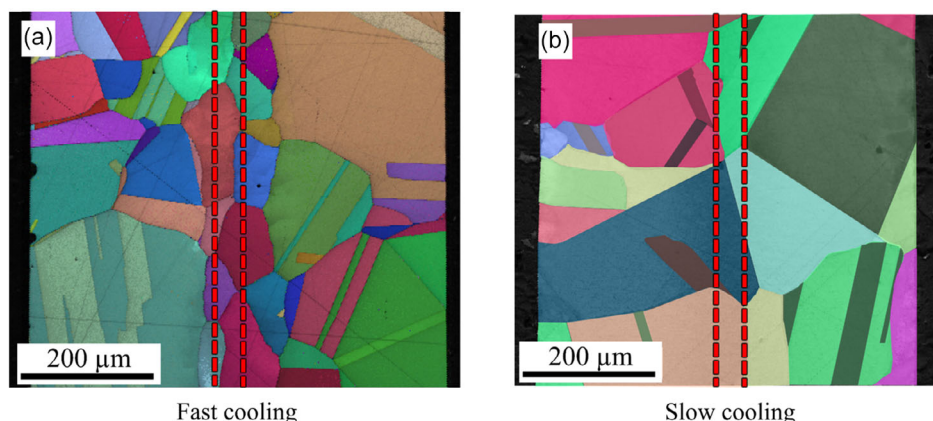


Figure 7. EBSD images after brazing with the CCA braze filler a) 1200 °C for 60 min and fast cooling and b) 1200 °C for 90 min and slow cooling. The red dashed lines indicate the initial thickness of the brazing foil.

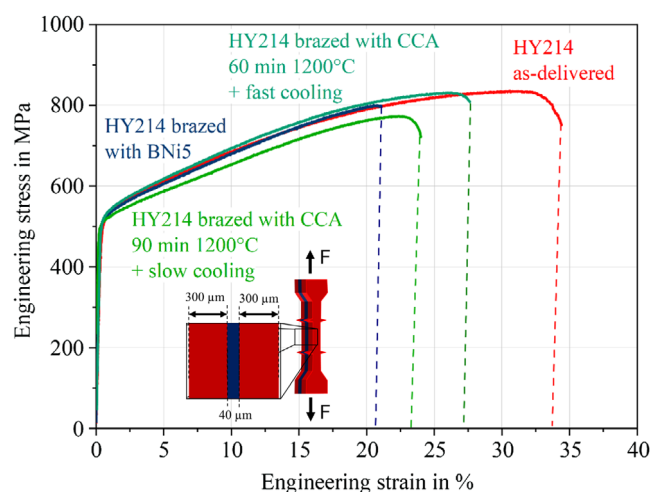


Figure 8. Stress-strain curves for the brazed samples and the Haynes 214 metal sheet (HY214 as delivered). A schematic detailing the specimen geometry is included in the figure, wherein the braze filler layer is shown in blue and the Haynes 214 base material in red.

Table 3. Ultimate tensile strength and elongation at fracture of the CCA brazed samples, the BNi-5 brazed reference samples, and the as-delivered Haynes 214 metal sheets.

	Ultimate tensile strength [MPa]	Elongation at fracture [%]
Haynes 214 brazed with CCA (fast-cooling)	820 ± 30	28 ± 3
Haynes 214 brazed with CCA (slow-cooling)	730 ± 20	24 ± 2
Haynes 214 brazed with BNi-5 (conventional) ^[5]	800 ± 20	18 ± 2
Haynes 214 as-delivered ^[5]	900 ± 15	36 ± 1

BNi-5 filler. Among the CCA brazes, the samples with fast cooling exhibit significantly higher ductility than the slow-cooled samples.

3.4. Wettability

Figure 9 shows the change of in situ contact angle measurements throughout the melting process. The measurement recording starts at a temperature ≈ 40 °C below the liquidus temperature. For both the CCA filler and the BNi-5 filler, the measurement begins with an almost rectangular cube and hence a contact angle of $\approx 90^\circ$. The onset of melting is indicated in **Figure 9**, occurring approximately at the 2 min mark. Interestingly, the wetting process of the Haynes 214 substrate with the BNi-5 filler is significantly slower than with CCA filler. Wetting with BNi-5 filler is completed ≈ 5 min after the start of melting. In contrast, wetting with the CCA filler is accomplished within 30 s. After wetting the Haynes 214 substrate, the contact angle of the CCA filler rises again.

Figure 10 shows a snapshot of the two filler materials at the 7 min mark. While BNi-5 forms a smooth elliptical surface, a structured rougher pattern emerges for the CCA filler.

Furthermore, the spreading area was determined after the brazing process. The spreading areas are very similar, indicating that the wettability on Haynes 214 is similar for both brazing materials.

3.5. Oxidation

The mass gain observed after oxidation experiments at 1000 °C for 168 h in air atmosphere averaged 0.40 mg cm^{-2} for the Haynes 214 sheets and 0.27 mg cm^{-2} for the sheets brazed with CCA filler. EDX measurements revealed the formation of an aluminum oxide scale on both Haynes 214 and the samples brazed with CCA filler material. The thickness of the oxide layer on the CCA sample ranged from 0.9 to $1.9 \mu\text{m}$, while the oxide layer thickness on the Haynes sample varied between 2.0 and $4.6 \mu\text{m}$.

4. Discussion

The MnFeCoNiCu CCA filler allows advantageous adjustment of the liquidus temperature. Thermo-Calc simulations using the TCNI12 database effectively simulate the liquidus and solidus

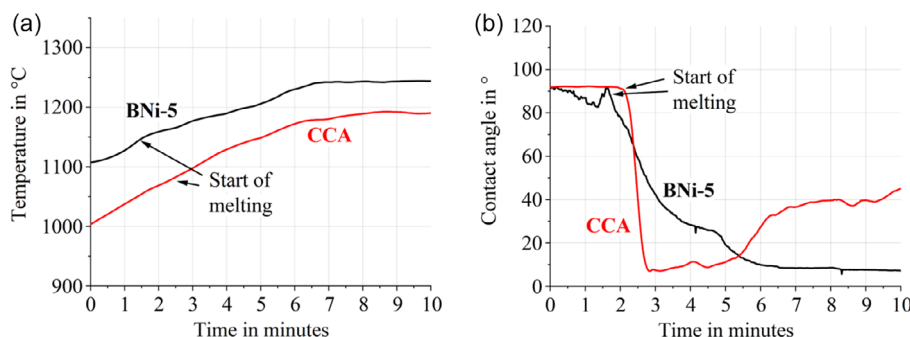


Figure 9. Contact angle measurements of Haynes 214 with BNi-5 (black) and CCA filler (red): a) Temperature profile and b) Evolution of the average contact angles of a cube made of during and after the melting process.



Figure 10. Image captured 5 minutes after the initiation of the melting process on a Haynes 214 substrate: a) BNi-5 filler and b) CCA filler. The yellow dashed lines indicate the baselines for the contact angle measurements.

temperatures of the CCA braze filler, closely matching experimental DSC data. This enables accurate predictions for composition and liquidus-temperature adjustments. For the $\text{Mn}_{33}\text{Cu}_{22}\text{Ni}_{20}\text{Co}_{20}\text{Fe}_5$ (in wt%) filler, the liquidus temperature is $\approx 1104^\circ\text{C}$. Therefore, lower brazing temperatures than 1200°C are possible when using the CCA filler, leading to a lower risk of deformation and reduced costs. The TCNI12 database is well suited for simulating composition profiles in the brazing joint (see Figure 5), indicating that rapid determination of brazing parameters for MnFeCoNiCu CCA fillers is possible with this database.

Metallic multicomponent alloys with evenly distributed alloy elements minimize the occurrence of phases by forming a random solid-solution structure due to increasing entropy.^[15–17] Studies by Gao et al.^[12] and Schneiderman et al.^[11] confirmed the presence of a FCC solid-solution structure in the as-cast $\text{Mn}_{33}\text{Cu}_{22}\text{Ni}_{20}\text{Co}_{20}\text{Fe}_5$ (in wt%) filler. The absence of brittle phases in the CCA filler is attributed to its single-phase solidification and its capacity to accommodate a broad range of compositions in a single-phase FCC solid solution. However, during the fast-cooling brazing process at 1200°C for 60 min, a segregation rich in manganese and copper was observed along the brazing centerline. This segregation has been observed in prior work on the CCA,^[10] and it can be homogenized with subsequent heat treatment. However, the segregation after the fast-cooling process has no negative effect on the mechanical properties.

The averaged elongation at fracture for the BNi-5 sample is 18%, and it is increased to 28% through the fast-cooling process with CCA filler. Although the elongation at fracture is still lower than that of the as-delivered Haynes 214 metal sheets (36%), the improvement is noteworthy. The absence of embrittling microconstituents enhanced the ductility of brazed sheets using the

CCA filler compared to those brazed with the reference filler BNi-5. For all brazes, the yield strength and strain hardening behavior remained close to the Haynes 214 base material, although a slight reduction in yield strength was observed for the slow-cooled (90 min duration) CCA braze, likely indicative of undesirable grain growth in the base material. The fast-cooled (60 min duration) CCA braze presented no reduction in yield strength or strain hardening rate. Based on the obtained insights, a brazing duration of less than 60 min at a brazing temperature of 1170°C is recommended. For Haynes 214 as the substrate, the fastest possible cooling rate to below 600°C is advised. The best mechanical properties were achieved with a cooling rate of $110^\circ\text{C min}^{-1}$. Temperatures below the solution heat-treating temperature of 955°C can lead to grain boundary carbide precipitation and the precipitation of the gamma prime phase in Haynes 214. Consequently, this makes Haynes 214 susceptible to strain-age cracking.^[2]

Despite the higher brazing temperature and longer duration, the grains in the samples produced with CCA filler are smaller than those in the BNi-5 reference sample. Small grains are observed along the brazing line in the fast-cooled CCA sample. Prior work indicates that these smaller centerline grains are due to dynamic recrystallization during cooling. A larger gradient in composition leads to increased lattice strain and an increased mismatch in the coefficient of thermal expansion, thus enhancing dynamic recrystallization. Dynamic recrystallization occurs during a temperature window where the braze is cool enough to have accumulated thermal stress by filler/substrate thermal-expansion mismatch and still hot enough for recrystallization.^[18]

The analysis of the wetting behavior reveals that the CCA filler extensively wets the Haynes 214 substrate, ensuring strong adhesion. The good wetting properties can be attributed to the chemical compatibility between the filler and substrate, as well as the surface energy properties of the MnFeCoNiCu CCA filler. Compared to the BNi-5 filler, the melting process with the CCA filler occurs more rapidly under the same heating rate. The contact angles at the end of the melting process are identical, small at around 6° for both braze filler alloys. While BNi-5 filler forms a smooth and elliptical surface, the CCA filler contracts and forms a rougher surface. This behavior can be attributed to the evaporation of manganese to the open environment during the wettability test. The vapor pressure of manganese is $\approx 80\text{ Pa}$ at 1200°C , which is significantly higher than the vacuum brazing pressure

of 10^{-2} Pa.^[19] When using the CCA braze filler alloy as a foil between two Haynes 214 sheets, no contraction of the braze material is observed, indicating no obvious Mn evaporation. This is because the braze filler alloy is not directly exposed to the environment and is evenly distributed by the applied load of 1 N. To prevent the evaporation of manganese, the CCA braze filler alloy could benefit from a protective gas atmosphere to supply pressure to inhibit Mn evaporation when brazing on exposed surfaces.

The oxidation properties of the Haynes 214 base material at 1000 °C are not affected by the CCA braze filler. The alumina layer on the CCA-brazed sample is slightly smaller than the oxide layer on the as-delivered Haynes 214 sample. As a result, the weight gain of the CCA-brazed sample is lower. Because the oxidation experiments were conducted in air at atmospheric pressure, which is well above the vapor pressure of Mn at 1000 °C, Mn evaporation and associated mass loss are unlikely to have conflated the mass gain measurements.

5. Conclusion

The CCA $\text{Mn}_{33}\text{Cu}_{22}\text{Ni}_{20}\text{Co}_{20}\text{Fe}_5$ (in wt%) can serve as an alternative to conventional nickel-based braze filler alloys with silicon as liquidus temperature depressing elements. It shows good wetting behavior on Haynes 214 metal sheets, similar to that of the Ni-base braze filler alloy BNi-5. Moreover, the mechanical properties of the samples brazed with CCA filler surpass those of the samples brazed with BNi-5. The exceptional tensile ductility of the CCA filler is attributed to its single-phase FCC microstructure and the absence of brittle phases. The ultimate tensile strength remains comparable to the BNi-5 brazed samples. Due to the inclusion of inexpensive elements such as Fe and Mn among the major CCA constituents, the estimated raw material cost of the CCA filler is $\approx 15\text{--}20\%$ less expensive than that of BNi-5. Thermo-Calc simulations using the nickel-based databases TCNI12 and MOBNi6 are effective in predicting the liquidus temperature of the CCA filler and the diffusion zones after the brazing process.

The recommended brazing process resulting from this work is: 1) braze filler material $\text{Mn}_{33}\text{Cu}_{22}\text{Ni}_{20}\text{Co}_{20}\text{Fe}_5$ (in wt%); 2) brazing at 1170 °C for 60 min; and 3) fastest possible cooling of $>110^\circ\text{C min}^{-1}$ down to 600 °C.

Acknowledgements

This work was supported by the Deutsche Forschungsgemeinschaft (DFG) in the context of the research projects GL 181/40-3, WE 2351/14-3, and BA 2848/5-3 and by the National Science Foundation under award no. 1847630 and award no. 2208777. The authors gratefully acknowledge Dr. Michael Sanders for his assistance with the DSC analysis.

Open Access funding enabled and organized by Projekt DEAL.

Conflict of Interest

The authors declare no conflict of interest.

Data Availability Statement

The data that support the findings of this study are available from the corresponding author upon reasonable request.

Keywords

brazing, Haynes 214, honeycombs, nickel-based superalloys

Received: March 25, 2024

Revised: May 31, 2024

Published online: June 16, 2024

- [1] H. L. Stocker, D. M. Cox, G. F. Holle, NASA CR-135307 (EDR 9339), 1977.
- [2] Haynes International, *Data Sheet Haynes 214* 2021.
- [3] D. R. Sporer, L. T. Shienbob, *Turbo Expo*, 2004, 4, 763.
- [4] The Prince & Izant Company, *Data Sheet AMS 4782 (BNi-5)*, 2021.
- [5] J. Vogler, J. Song, J. Huber, R. Völkl, U. Glatzel, in *Proc. 10th Inter. Symp. Superalloy 718 Derivatives*, Springer Nature, Cham, Switzerland 2023, p. 445.
- [6] X. Huang, W. Miglietti, *J. Eng. Gas Turb. Power* 2012, 134, 10801.
- [7] S. K. Tung, L. C. Lim, M. O. Lai, *Scr. Metall. Mater.* 1995, 33, 1253.
- [8] S. Ulan kzy, R. Völkl, O. Munz, T. Fischer, S. Welzenbach, U. Glatzel, *Mater. Sci. Technol.* 2019, 36, 1012.
- [9] S. Ulan kzy, R. Völkl, O. Munz, T. Fischer, U. Glatzel, *J. Mater. Eng. Perform.* 2019, 28, 1909.
- [10] B. Schneiderman, A. Hansen, A. C. Chuang, Z. Yu, *J. Manuf. Process.* 2023, 87, 25.
- [11] B. Schneiderman, O. Denonno, J. Klemm-Toole, Z. Yu, *Welding J.* 2022, 101, 85.
- [12] M. Gao, B. Schneiderman, S. M. Gilbert, Z. Yu, *Metall. Mater. Trans. A* 2019, 50, 5117.
- [13] M. van Gorcum, *Python Sessile Drop Analysis*, <https://github.com/mvgorcum/Sessile.drop.analysis> (accessed: January 2024).
- [14] J. O. Andersson, T. Helander, L. Höglund, P. Shi, B. Sundman, *Calphad* 2002, 26, 273.
- [15] W. Tillmann, T. Ulitzka, L. Wojarski, M. Manka, H. Ulitzka, D. Wagstyl, *Weld World* 2020, 64, 201.
- [16] B. Cantor, I. Chang, P. Knight, A. Vincent, *Mater. Sci. Eng. A* 2004, 375, 213.
- [17] L. X. Zhang, J. M. Shi, H. W. Li, X. Y. Tian, J. C. Feng, *Mater. Des.* 2016, 97, 230.
- [18] B. Schneiderman, *M.S. Thesis*, Colorado School of Mines 2020.
- [19] C. B. Alcock, V. P. Itkin, M. K. Horrigan, *Can Metall. Quart.* 1984, 23, 309.